TBM Tunnelling under Difficult Conditions: Too Massive, Too Faulted, Too Wet, Too Deep

N.R.Barton
NB&A, Oslo, Norway

ABSTRACT: It is common knowledge that TBM are remarkable machines. It nevertheless takes mental effort to accept that they can have world record 1 day, 1 week and 1 month tunnel advance as high as 172m, 703m and 2163m. However, the best monthly project averages for the usually smaller 3m to 6m diameter machines which have delivered these incredible records are 'only' 1.1 to 1.3 km, not anywhere near 2km. In other words, tunnel length and time take a toll, due both to geology, hydrogeology, and machine-related delays. Unfortunately, the other side of the coin has seen more than a few TBM that remain buried in mountains forever (needing drill-and-blast completion), or they are delayed for many months or even years. This huge range of performance demands a lot from models of TBM prognosis: the range of tunnel advance may vary over four orders of magnitude from 0.001m/hr (i.e. stuck in fault zone) to an occasional 10m/hr penetration rate. Because of the huge range of an empirical parameter $Q_{TBM,}$ this range is possible to encompass, and is founded on the 0.001-1000 Q-value range, plus particular emphasis on comparing cutter thrust and rock mass strength, 1 to 100MPa.

1 INTRODUCTION – WORLD RECORDS

TBM prognosis models must be capable of explaining less than 1m/hr penetration rate (PR) in hard massive rock, perhaps short-term 10m/hr penetration rate (PR) in softer jointed rock, but only 0.01 m/hr average advance rate (AR) when severely delayed in fault zones. The implied eighty meters during one year, struggling to get through a faulted zone is clearly close to the limit of acceptance. Values an order of magnitude lower than this mean virtual burial. So we see in these figures a ten thousand-fold variation (fastest 10m/hr, slowest 0.001m/hr) that needs a geo-technical, quantifiable explanation.

In this lecture we will examine the adverse effects of massive hard rock, faulted rock with and without the complications of wet tunnels requiring delaying pre-injection, and finally TBM tunnels that are actually too deep in relation to the strength of the rock, and therefore suffer rock bursts.

Thanks to some detailed TBM world record advance rate statistics provided by Robbins on the internet, it was possible to derive the present (2015) record data shown in Figure 1. The 3 to 6m diameter class shown with the smallest 'cubes' is *the mean of three sets* of data given for 3-4m, 4-5m and 5-6m TBM, based on assumed 24 hours, 168 hours and 720 hours. The 6 to10m diameter class shown with the larger 'cubes' is *the mean of four sets* of data for 6-7m, 7-8m, 8-9m and 9-10m TBM. This collective averaging helps to see trends more clearly.

In Figure 1, day, week and month records (given in meters) are converted to the form AR (m/hr) by dividing by 24, 168 and 720 hours. Data from 8 countries are represented, but chiefly USA and China. The record *mean monthly* data plots at AR = 1.7 m/hr for the 3m to 6m class, and at AR = 1.1 m/hr for the 6m to 10m class. These results are shown with the two small circles. The larger crossed-circle to the right represents 54 weeks for 5.8 km at the Svea Mine Access Tunnel, achieved during the LNS drill-and-blast world record. This was driven in coal-measure rocks and obviously required some shotcreting and rock bolting, due to varied Q-values. Slowest progress was made through a near-surface zone of permafrost.

2 CASE RECORDS SHOW DECELERATION

There is an all too common habit of reporting utilization (U) of TBM without specifying the time period involved. An estimated average daily utilization is especially an insufficient form of prognosis. Since stand-stills are naturally excluded, the client may get an optimistic view of likely performance. Utilization is estimated from the classic and most used TBM

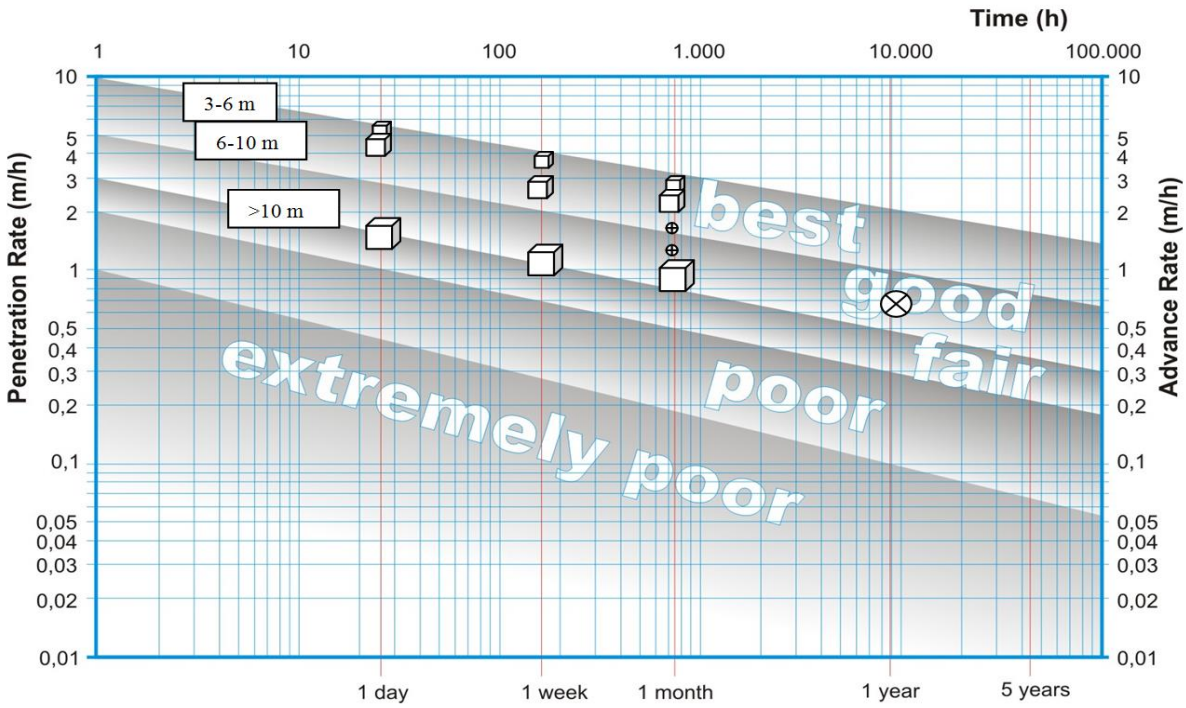

Figure 1**.** Using a log-log-log plot of PR (penetration rate, left axis only) and AR (advance rate in remainder of plotted area) and time T (total hours), the synthesized **present world-record data** for different sizes of TBM is shown, based on data provided by Robbins web-site (Barton, 2013). Most of the world records also belong to Robbins TBM.

.

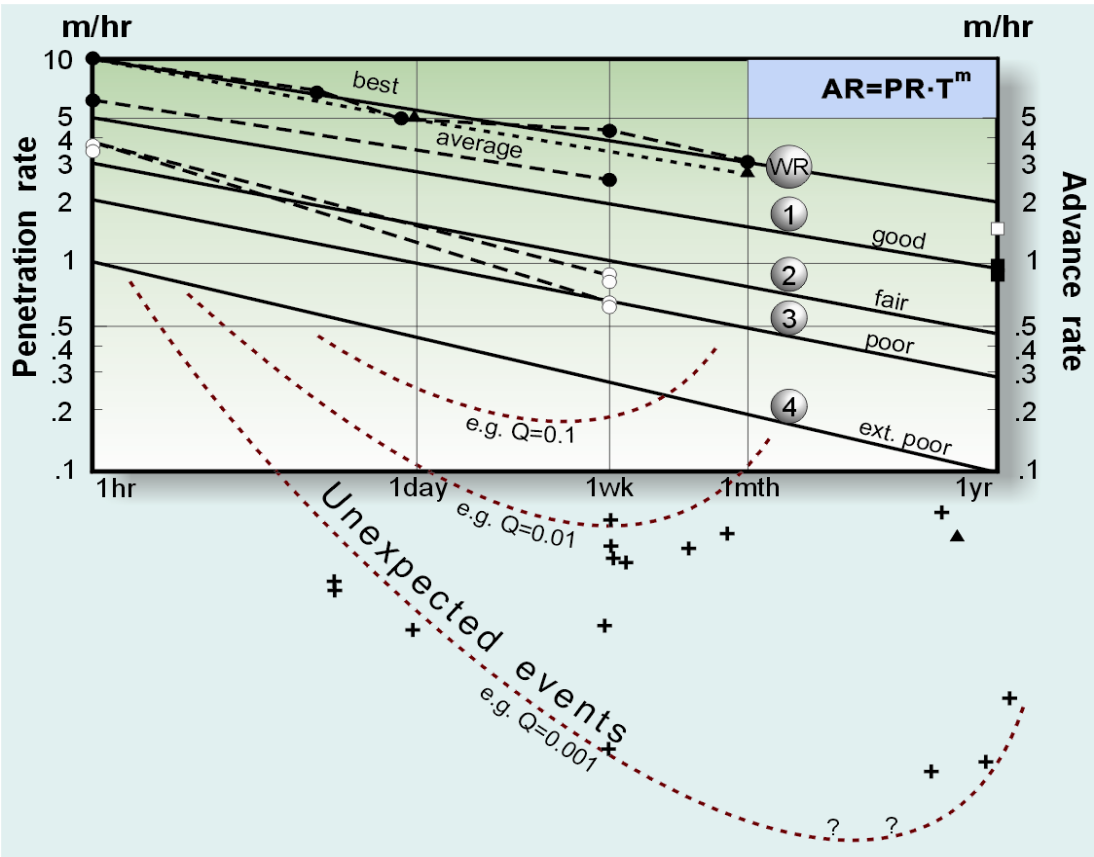

Figure 2. Trends from open-gripper case records representing 145 lengths of well-characterised TBM tunnels, totalling approximately 1000km of tunneling. The performance is represented by log PR – log T – log AR. The PR value applies only to the left axis. T (total hours) and AR occupy the remainder of the diagram. Adjectives clearly apply to smaller, faster TBM. (Barton, 2000). Note that AR = PR x U has been improved to a time-dependent AR = PR x T^m. Gradients (-)m, of each line have units LT^{-2} (i.e. deceleration). See Table 1 for (-)m values.

performance equation:

$$AR = PR \times U \quad (1)$$

where AR = (actual) advance rate in m/hr, and PR = penetration rate (for uninterrupted boring) in m/hr. U is the fraction of time when boring occurs, as seen on the traditional 'pie- or pizza-diagram'. For convenience U is usually expressed (in speech) as a percentage. Note that in Figure 2, U has been expressed as T^m. This is explained in Table 1 and is also shown in Figure 2 (top-right corner).

The five typical 'lines' of performance in Figure 2 are the same as shown in Figure 1. The hand-drawn sources of these smoothed data were originally given in Barton (2000). The 'unexpected event' curves (and crosses) in Figure 2, are the low-Q-value-linked worst cases, with (in 2000) three documented permanent TBM burials in the case of older, poorly equipped TBM. There are of course many more buried cases.

As illustrated by the world records of Figure 1, and as illustrated by 1000 km of mostly open-gripper case records, summarized in Figure 2, there is actually a time-dependent element in U which is conveniently ignored in a remarkable number of tunnel magazine articles and also in commercial TBM prognoses.

conditions and use of moderate thrust, the deceleration gradient (-) m varied from (-) 0.16 to (-) 0.31 for both tunnels. However, (-) m was (-) 0.38 during the learning curve, and (-) 0.33 when exiting through bad ground. Due to risk of methane gas, operation was always in closed mode, which of course increases delay and makes (-) m more steeply negative. The mean cutter forces used in the weak sandstone and conglomerate/clay were 16.9 and 10.3 tons, which explains the low PR with moderate UCS.

Since a client pays for a completed tunnel, a false impression of actual hours (T) is obtained if inevitable standstills, such as in untreated fault zones, are *excluded*. 'Waiting for the train' or broken conveyor belts due to blocky rock may be part of the recorded experience, which cannot be ignored in the prognosis of long TBM tunnels. There are approximately 24 x 7 x 50 ≈ 8700 hours of potential three-shifts of work in one year, and during TBM standstills the clock is still running, with the tunnel completion date likely delayed. Many TBM projects come in 'late' due to ignorance of this element of time / length. So, risk (of cost and time over-run) can be reduced by using T^m in place of a potentially misleading U. A 'monthly utilization of 30%' does not give the correct time for tunnel completion, even if a mean PR of say 3m/hr was quite representative for the whole tunnel. When

Table 1. Deceleration gradients (-m) for the five trends-of-performance lines in Figure 2, based on 145 cases totalling 1,000 km of mostly open-gripper TBM, from Barton, 2000. A specific 56 km of double-shield performance (two Wirth TBM, two Herrenknecht TBM) is also indicated. Roughly half the deceleration gradient is seen, but double-shield are not always so good.

Performance Line #	Description (refer to Figure 2)	Deceleration gradient *(-) m* (units of LT^{-2})
WR	World records	-0.13 to -0.17
1	Good,	-0.17,
2	Fair	-0.19
3	Poor,	-0.21,
4	Extremely Poor	-0.25
Double-shield	Poor PR increasing to Good AR	-0.08 to -0.12

A large-diameter EPB machine may apparently triple these double-shield (harder rock) gradients for obvious reasons related with the greater challenge of maintaining semi-continuous face support. (Barbieri et al. 2013, Tanzini pers. comm.)

In Figure 3, the performance of a large EPB (earth pressure balance) machine is shown. There were 78 disc cutters due to significant sandstone and conglomerate sections of the tunnels, in addition to the numerous soft ground picks. Note that the range of PR was mostly 1 to 2 m/hr, and due to difficult

U is replaced by T^m, more realistic and more reliable (trust-worthy) TBM prognoses are obtained.

3 Q-VALUES AND TBM PERFORMANCE

When a TBM tunnel is driven in one predominant rock type, such as the case of 5 km through granites in Malaysia, described by Sundarem and Rafek (1998), there is a surprisingly good correlation of penetration rates (PR) with the Q-value, and with even simpler measures of jointing, such as the volumetric

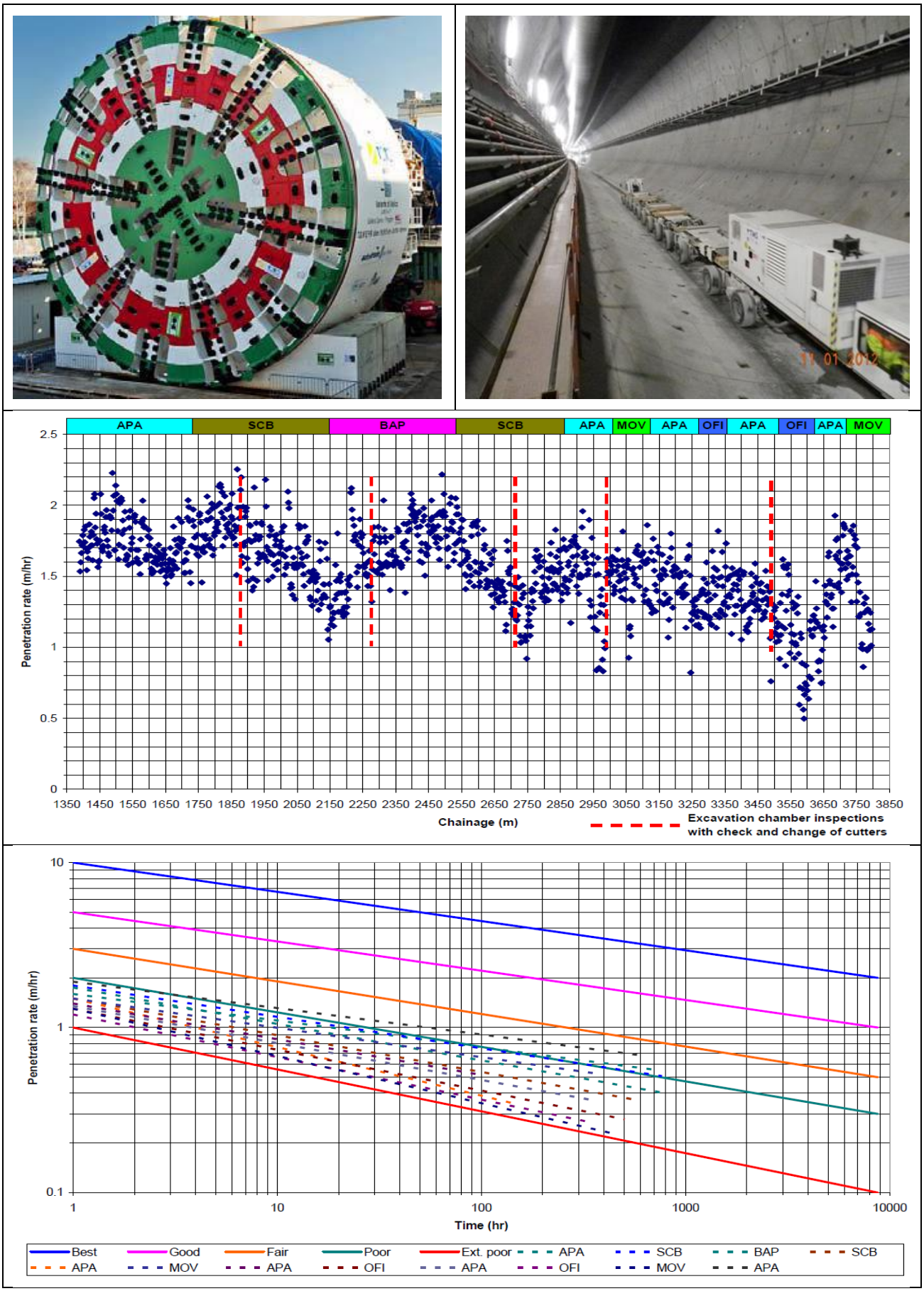

Figure 3. Sparvo Tunnel, driven by the world's (now only) second largest EPB (earth pressure balance) TBM of 15.6 m diameter has twin tunnels of 2.6 km length. These performance lines match the decelerations described above, though are of course more steeply inclined and have lower PR. (Barbieri et al. 2013, Tanzini pers. comm.)

joint count, and even with mean joint spacing. (Such 'simplicity is because other 'necessary' parameters such as rock strength and abrasivity are 'constant' in the continuous granite).

The Q-data PR-correlation shown in Figure 4 is based on 2,825m of data, for medium to coarse grained granites with UCS in the range 130 to 246 MPa (mean 182 MPa). This is similar to that expected in the four-TBM, total 2 x 19km Follobanen Oslo-Ski project, also mostly driven through granites, and granitic gneiss, which will be described later as an example of Q_{TBM} prognosis.

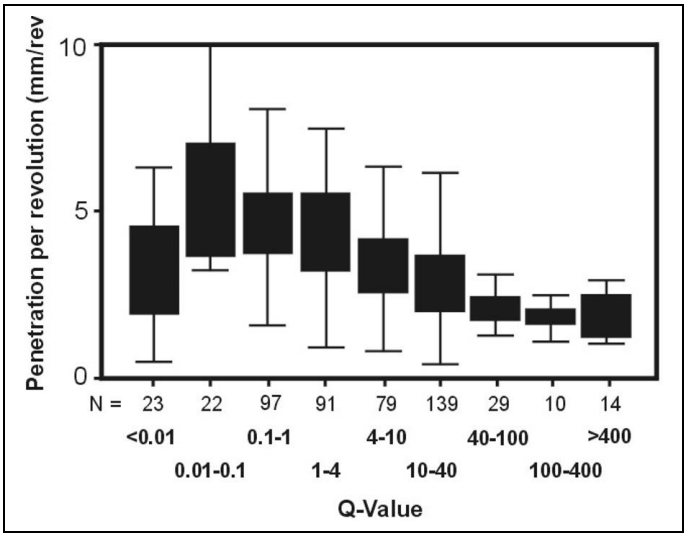

Figure 4. In a project involving only granite, as illustrated here, consistent correlation of penetration rate with Q-values (using mean Jr/Ja) is seen. (Sundarem and Rafek 1998). Note the matching PR trend in Figure 6.

It was found by Sundaram and Rafek (1998) that the *average* Jr/Ja ratio (joint roughness/joint alteration-filling ratings in the Q-value) gave a better correlation of PR to Q than the 'most adverse' Jr/Ja ratio, as traditionally used when selecting suggested tunnel support and reinforcement for single-shell NMT (Norwegian Method of Tunnelling) (Barton and Grimstad, 2014).

When logging more than 300 rock exposures and seven cores drilled through weakness zones as input to Follobanen Oslo-Ski prognoses, the writer also logged all the principal Jr/Ja ratios in the form of Q-histograms. This Q_{TBM} study was described by Barton and Gammelsæter (2010). An example is given later.

4 CUTTER LIFE AND THE EFFECT OF HIGH Q-VALUES AND HIGH STRESS

Manufacturers of new TBM like to claim that their 'cross-over' or 'all conditions' tunneling machines can tackle all conditions and should be selected instead of drill-and-blast, 'because the tunnel is so long', and nowadays even use the argument 'because the conditions are so bad'. This double optimism may not be justified by actual experiences, nor can it be-satisfied by the numerous older TBM still in use.

As we will see later, and as hinted at by the natural *decelerations* seen in Figures 1 and 2, the *long tunnel argument* is inviting risk, even though the ventilation aspect for the long tunnel may weigh heavily in favour of TBM. However, in terms of geotechnical risks, great care is needed before selecting TBM for the long, and probably poorly explored deep tunnel. The prospect of good quality rock may not favour TBM if there is too little jointing and also very high cover, (i.e. 'too deep' for TBM) as illustrated later.

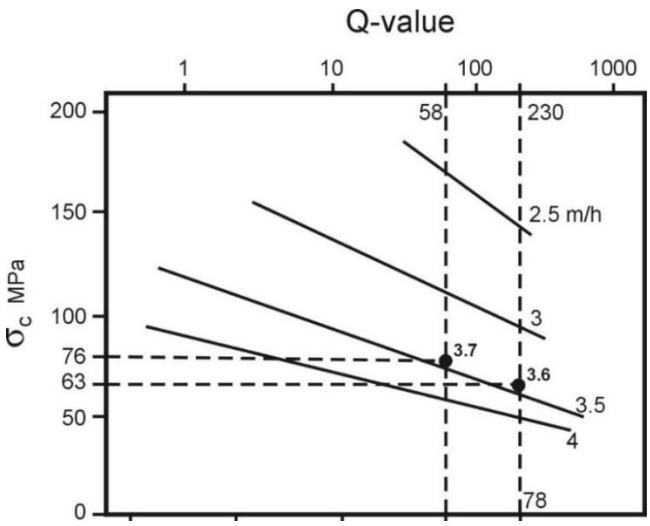

Figure 5**.** There is a logical correlation between penetration rate (given here in m/hr) and the Q-value. Massive high-Q rock slows progress, and if UCS (σ_c) is also high, an even slower penetration rate is inevitable. Low UCS and low Q-value (but not too low) are positive, as in the left-hand bottom corner. Modified (without RSR scale), from Innaurato et al. (1991).

The adverse nature of *massive rock* with insufficient jointing, especially when this is combined with high UCS and high abrasiveness is typified by the need to change cutters on average every 1 to 2m. In practice this means many hours boring with an increasing number of ineffective cutters, because the 5 to 10 (or more) cutters may not be changed until the once-per-24-hours maintenance shift. By then there might be some cutters with 'flats' which consequently have ceased to rotate. So each 24hr period may experience reducing advance rate (AR) if cutter-change needs are significant. This is a contractor's nightmare.

Figure 6 indicates 'lack of joints' (despite 'no support area') in the area of ultra-high Q-values. In cases known to the writer, extremely high RMR (> 80) and Q-values (>100) are sometimes so consistent in the virtual absence of jointing, that a contract may fall far behind expectations. In such cases 'expectations' are sometimes based on 'artificially jointed' core taken conveniently, near the planned

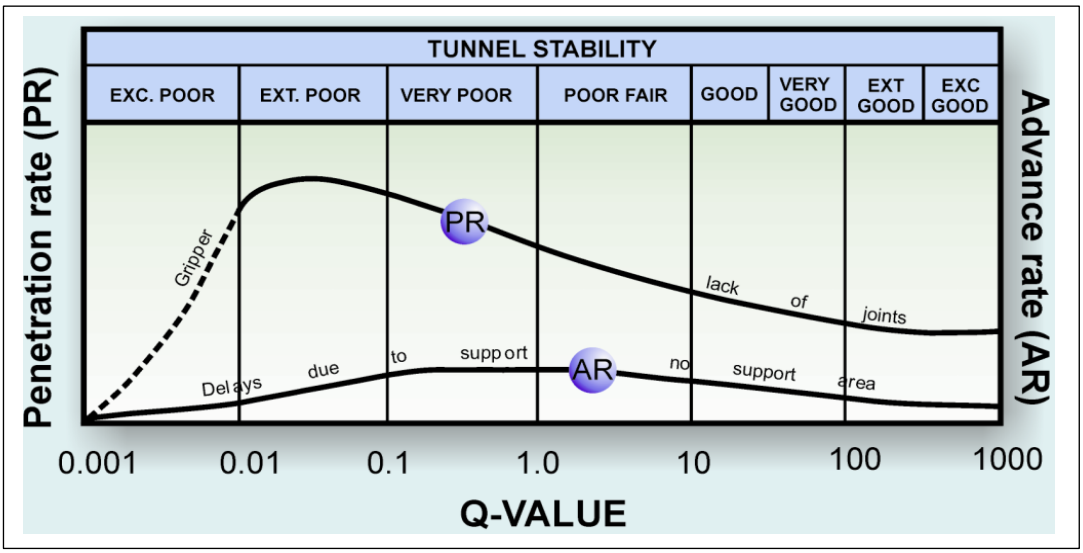

Figure 6. This figure shows, in principle, how penetration rate (PR) and advance rate (AR) are likely to vary with the regular Q-value. Note the increased ratio of PR/AR (in other words reduced utilization U) towards each end of the Q-scale. It will be realized that the original Q 'adjectives' (poor, fair, good etc) need modification for TBM: as in Figure 7 below.

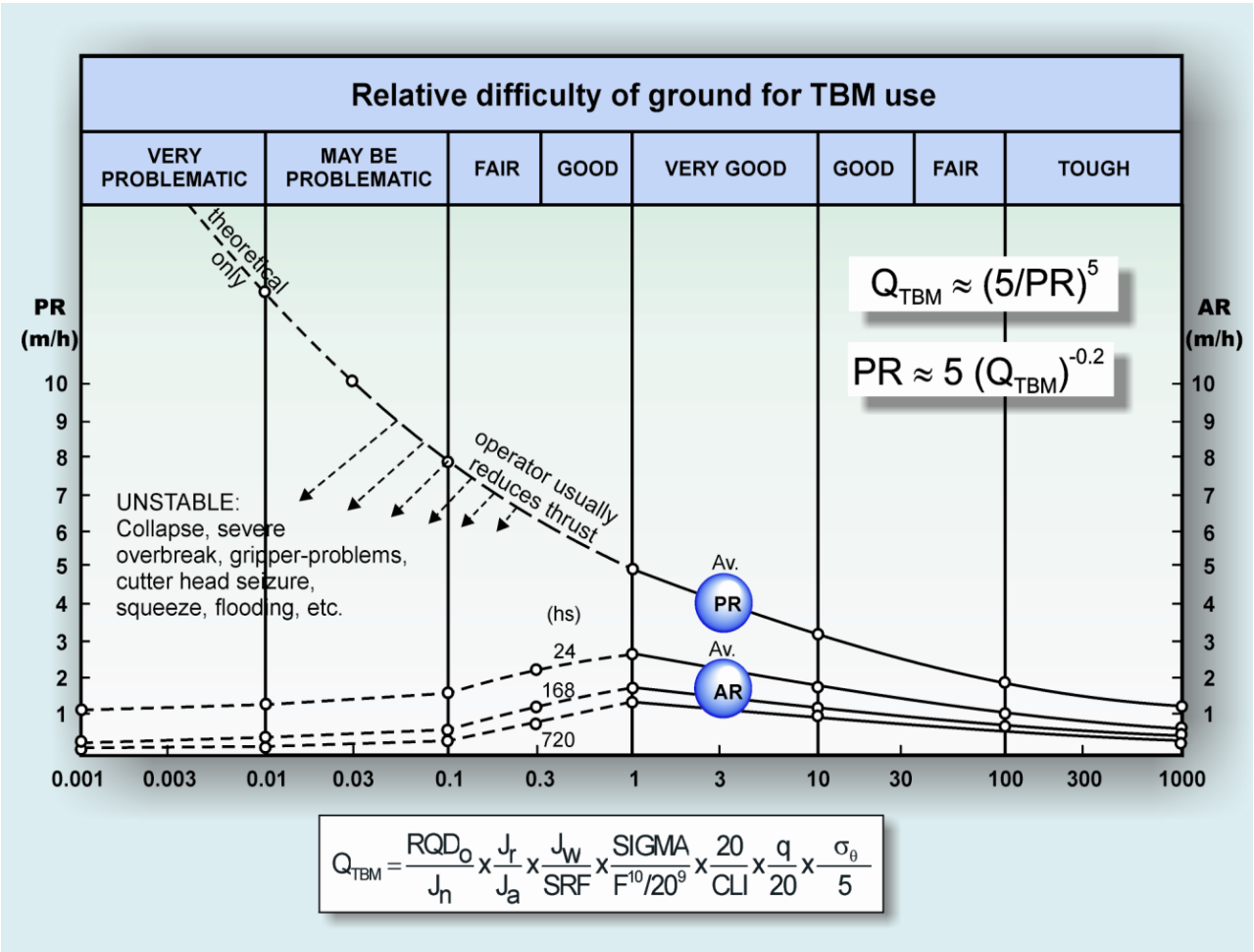

Figure 7. This figure introduces the multi-component machine-rock parameter Q_{TBM}, which uses the six Q-parameters for rock mass description, and has extra parameters such as cutter force and rock mass strength when describing TBM performance. Note the more relevant adjectives. Here we see the effect of: 'too faulted', 'too massive' as in the title of this paper. F = mean cutter force (tons) normalized by 20tons. SIGMA is an approximate estimate of rock mass strength = $5\gamma Q_c^{1/3}$ (usually between 1 and 100 MPa). CLI = cutter life index (NTNU, 1998), q = quartz content normalized by 20%, σ_θ is an estimate of the biaxial stress at the tunnel face: approximately 5MPa per 100m increase of depth i.e. approx. 2 γH/100 or twice the vertical stress (based on $3\sigma_1 - \sigma_3$). In other words – up until stress/strain fracturing (this unfortunately needing support), boring becomes more difficult as tunnel depth increases.

tunnel portal, with no indications of the massive nature of the mountainous region to be traversed.

The all-round optimism from Owner, Contractor and Consultant may not be qualified by the sobering results of high-velocity V_P (such as 5.5 and 6.0 km/s) because dense rain forest makes such acquistion too difficult, and anyway the tunnel is 300 to 500m deep where the shallow refraction seismic might have been performed. So the TBM progresses at 10 to 15m/day and the optimistic 400m/month prognosis is also ahead of the reality.

Aside from the dilemma of increased cutter wear and damaged cutter-bearings, the application of high thrust, when available, is also counteracted by the adverse effect of confining stress (e.g. ≈ 5MPa/100m).

5 Q_{TBM} PROGNOSIS METHOD

The case-record basis for the development of a TBM prognosis model, detailed stage-by-stage in Barton (2000), later resulted in a user friendly computer program, which was termed Q_{TBM} in Barton and Abrahão (2003). This indeed employs the Q-system, but modified to an oriented Q_o format. RQD needs to be interpreted with respect to tunnel orientation (i.e. horizontal) and is therefore written as RQD_o. A 'conventional' vertical core can give a false high value of RQD (in relation to a low value in the tunneling direction), if there is a strongly oriented steeply dipping structure such as bedding or foliation.

For estimating Q_o, all joint sets are sampled regarding Jr/Ja, unless a particular set is assisting or hindering penetration. It is then allowed to influence the oriented Q_o - value more strongly. A convenient way to gather data is to log rock exposures like recent road cuttings (if available, and not heavily weathered), logging along imaginary horizontal scan-lines. Histogram-based recording of data allows thousands of recordings to be made rapidly. Examples for the Follobanen Oslo-Ski project were given in Barton and Gammelsæter (2010). One will be shown later.

Note that the lower set of curves in Figure 7, representing AR estimation for 24 hrs, 1 week, and 1 month are separated, because of declining utilization. Note also the new 'adjectives' (tough, problematic etc) specifically for TBM. It is clear that central Q_{TBM} values of ≈ 0.3 to 30 would be ideal for fast progress.

One of the most important normalized parameters in Q_{TBM} is mean cutter thrust (F, tons) which is normalized by 20 tons. Greater or lesser applied thrust is then compared with SIGMA (rock mass strength estimate = $5\gamma Q_c^{1/3}$) where $Q_c = Q_0$ x UCS/100 and γ = density in gm/cm^3. For most conceivable rock masses, SIGMA ranges from 1 to 100 MPa, but in saprolite SIGMA < 1 MPa. The resulting formula for PR (see top-right inset in Figure 7) which is strongly dependent on cutter thrust compared to rock mass strength, has been tested on numerous occasions, both for high-powered TBM with F > 30tons, and for blind-hole shaft drilling with F as low as 7 to 8tons. Realistic values of PR are obtained in each case, when the method is correctly used.

In essence, we allow the Q-value to assist in determining delays due to support requirements (it therefore effects – where appropriate - the *deceleration gradient -m)* and therefore overall AR. Furthermore, we allow the Q-value, and critical *rock-cutter*, and *rock mass-machine* parameters to *also determine* the speed of cutting (therefore effecting slower or faster PR). These dual roles of Q have been criticized, but empirically speaking the method works well. Figure 8 shows an example of a Q_{TBM} data-input screen. The parameters used in the simple (tabulated) calculations appear in the x-axis equation of Figure 7.

6 FAULT AND WEAKNESS ZONES

The fundamental difficulties of tunneling through fault zones, and prognosis-modeling this successfully, will be summarized later, by combining three extremely simple equations. They provide, when combined and presented in terms of time T, a convincing explanation of why so much time can be lost in an unexpected, and therefore usually untreated fault zone.

The key to this understanding is that the universal but variable deceleration gradient (-*m*) is strongly linked to low Q-values. Low Q-values and high negative deceleration gradients (meaning low utilization) go hand-in-hand. U cannot be independent of time T, as clearly shown in Figures 1 and 2, both for extremely fast and slower TBM tunneling.

Before presenting the three equations, it may be helpful to see how fault zones plot on the *log PR – log T – log AR diagram*, which was used as an introduction to the world records shown in Figure 1. Fault zones in general have a potentially delaying effect on overall tunneling rate. Their low Q-values usually demand heavier local support (or some difficulties with PC-element ring building due to over-break), so a steeper deceleration gradient is usually involved.

On the other hand, they may often (though not always) be 'easily' bored through using low cutter thrust, but probably need increased torque, since an unusual amount of intimate contact with the cutter-head is occurring. Unless blocks dislodge and jam the cutter-head, as may sometimes happen in unexplored mountainous terrain, the moderate delays may appear as shown in Figure 9. Only one of the steeply inclined lines suggests a delay of (>) 1 week.

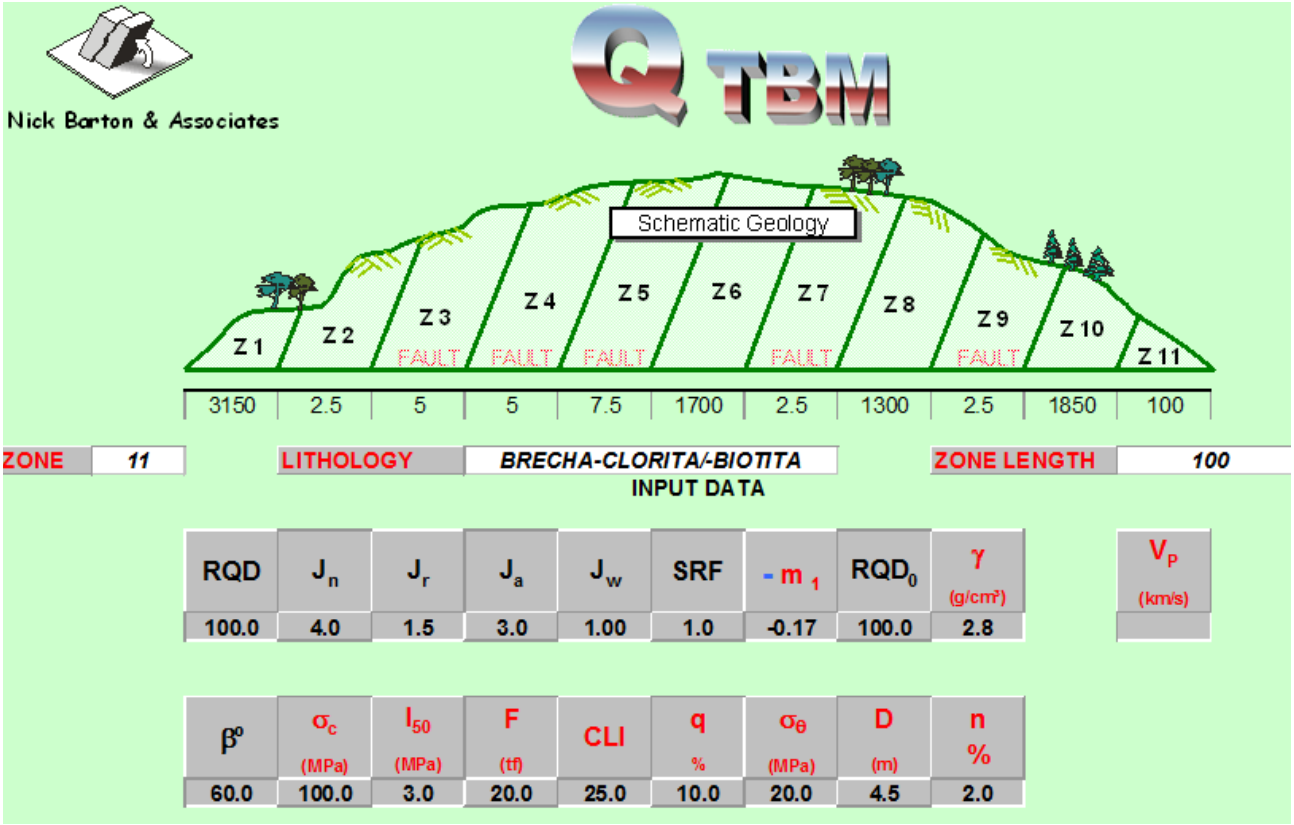

Figure 8. Based on the back-analysis of numerous open-gripper TBM case records (approx. 1,000km of tunneling), Barton (2000) developed simple empirical equations for the prognosis of PR, AR and T. In a valuable cooperation with a Brazilian geologist, the Q_{TBM} prognosis model was developed. (Barton and Abrahão 2003). This figure is an example of the input data screen, for a mine-access tunnel in Chile.

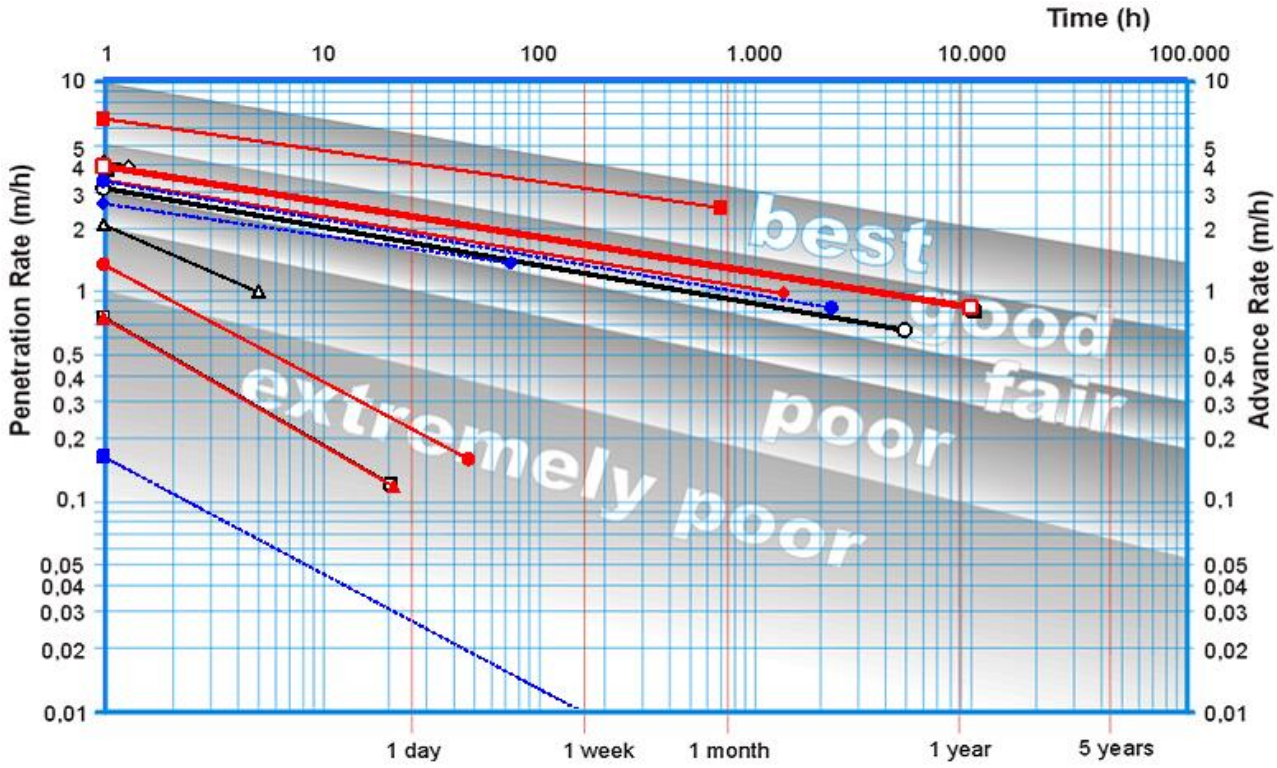

Figure 9. This figure graphs the predicted PR for different rock mass classes on the left-hand axis. The sloping lines, with gradients (-m) estimated via Q-values and additional machine-rock parameters, end after a predicted time interval, at specific values of AR. Overall: T = 10,000 hours, AR = 0.8m/hr (see thick, weighted-mean red line).

A weighted mean of about 10,000 hours for 8 km of tunnelling was predicted for this double-shield TBM (Figures 8 and 9), by combining the weighted mean of all of the eleven zones modelled. In practice it took longer due to unanticipated local labour practices (lunch-break outside tunnel in mining camp), and due to a long delay out of the starting chamber, where unexplored faulted rock was immediately encountered, and over-boring and cutter-head blockage were intermittently experienced for several weeks.

Double-shield TBM with push-off liner capabilities may get severely delayed if a fault zone is serious, as over-boring (void development in front of, to one side, or above the cutter-head) can just as easily develop ahead of these machines as ahead of open-gripper TBM, unless pre-injection in the one case, or spiling has been performed.

When faults are encountered deep below the water-table, and delay TBM progress, inflow of water may occur in an uncontrolled manner and for too long, with groundwater drawdown (and subsidence damage) as a likely result in the case of shallow tunnels beneath towns.

Risk analysis should address such consequences and their mitigation. It will not be sufficient to have gasketted PC-elements ready to be installed, while the next 15m of slow advance is negotiated before reaching the element erector. In this sense TBM can be 'too long'. Pre-injection would have been the solution. In the meantime, nearby monitoring wells may be registering groundwater drawdown, sometimes to great distances (0.5km, 1.0km, even 2.9 km are known).

6.1 *Fault-zone delays simply explained*

We need three basic equations to understand potential delays in fault zones. (The following nomenclature will be used as before: AR= advance rate, PR= penetration rate, U= utilization, expressed as a fraction, for any chosen *total time* T in hours).

Firstly:

$$AR = PR \times U \qquad (1)$$

(All TBM must follow this first equation, which was presented at the start of this article).

$$U = T^m \qquad (2)$$

(Due to the reducing utilization with time, advance rate decelerates, see Figs 1 and 2).

$$T = L / AR \qquad (3)$$

(Obviously time needed for advancing length L must be equal to L/AR)

With *continuous* boring T = L/PR, and in fact this simple equation also applies to walking. All readers can agree that these are very simple equations, and also empirically correct equations. But who has seen them combined and employed in prognosis?

By simple substitution we have the following:

$$T = L / (PR \times T^m)$$

(Here, T appears on both sides of equation: the final expression for T is therefore:)

$$T=(L/PR)^{1/(1+m)} \qquad (4)$$

This is a very important equation for TBM, if one accepts the case record evidence that *(-) m* is strongly related to low Q-values in fault zones and significant weakness zones. It is important because very *negative (-) m* values make the component ($^{1/(1+m)}$) *too big*. If the fault zone is wide (large L) and PR is low (grippers inefficient, water problems etc.) then L/PR may get too big to tolerate a big component ($^{1/(1+m)}$) in equation 4. Figure 12 is an example of application.

It is easy (in fact much too easy) to calculate an almost 'infinite' time for a fault zone using this 'theo-empirical' equation. The writer knows of four permanently buried, usually fault-destroyed, occasionally rock-burst destroyed TBM (Pont Ventoux, Dul Hasti, Pinglin, Jinping II). There are certainly many more, and the causes may be related to equation 4 logic. Extreme water or debris inflow, such as in karst can also imply extremely adverse Q-values. Delays can be counted in years, on occasion.

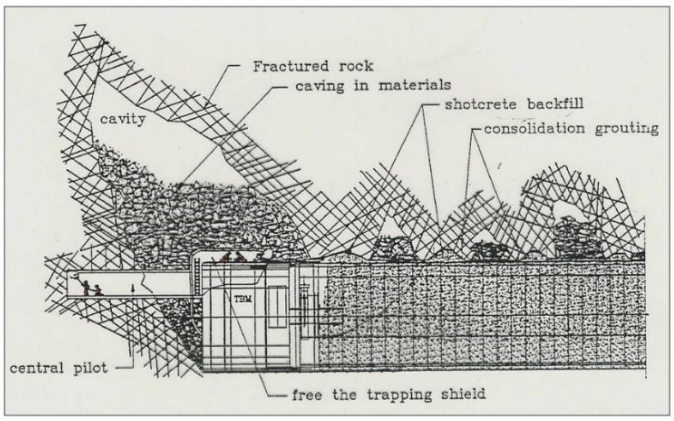

Figure 10. Exceptional problems in faulted meta-sandstones, with the need for a by-pass and top-heading to release the cutter-head. (Shen et al. 1999). Such stoppages occasionally provided the opportunity for replacing cutter-head 'armour' which was worn out every 4 to 5 km. One of these situations was observed by the writer. Pinglin road tunnels, Taiwan. Many fatalities.

Fault zones (and extreme stress/strength ratios causing rock bursts) will remain a serious threat to

TBM tunneling as we know it, unless the extremely poor rock mass qualities associated with fault zones can be improved by *drainage and pre-grouting*, specifically where Q < 0.1. There are signs that some TBM are being sufficiently equipped with holes through the front shield for pre-injection. This obvious need seems to have taken several decades to materialize in TBM-manufacturing practice.

Figure 11 illustrates how an experienced TBM contractor unfortunately made an adverse withdrawal of a TBM in order to treat a faulted zone which had stopped tunneling. (See CH. 2241 in both drawings). The resulting unloading of the fault (in sandstone/marl) seems to have caused deterioration of 'properties', and an undesirable worsening of the situation. Figure 13 suggests a possible reason using V_P.

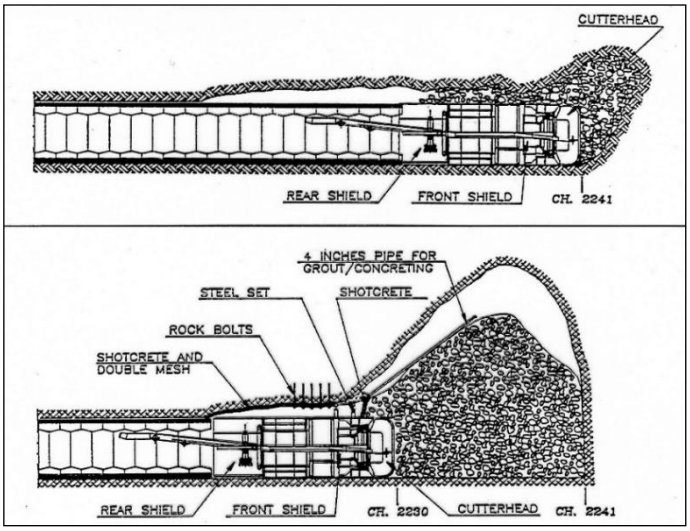

Figure 11. Adverse withdrawl of TBM in a fault zone. Evinos-Mornos water tunnel, Greece. Grandori et al. (1995)

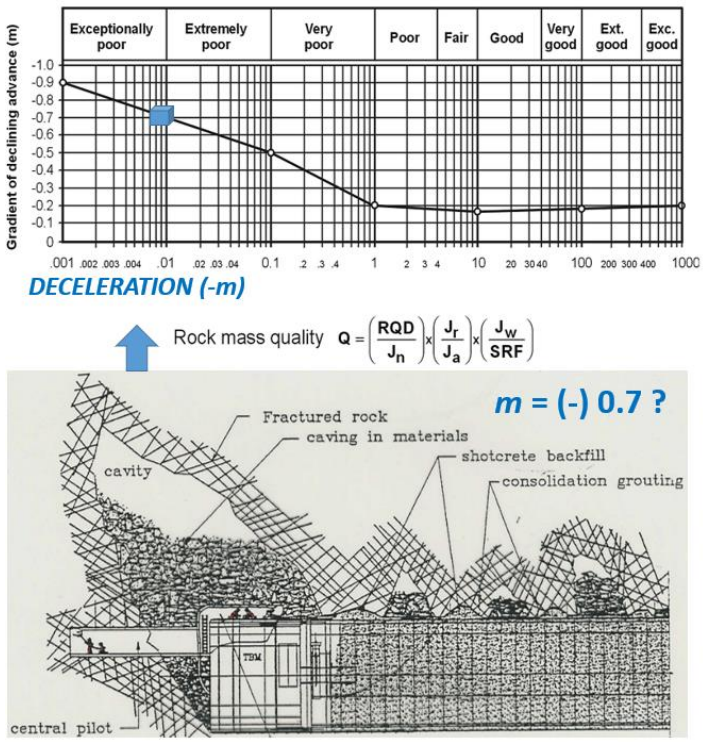

1. AR = PR x U
(All TBM must follow this).

2. U = T^m
(***Reducing utilization with time,***
time T must always be quoted!

3. T = L / AR
Time T for advancing length L.
(**Also applies to walking!**)

4. T = $(L/PR)^{1/(1+m)}$
THIS IS (-ve) !!

➢ ***1/(1+m)*** **= 1/(1-0.7) = 1 / 0.3 = 3.3!**

Figure 12. The correlation of very low Q-values and severely delayed TBM was demonstrated in Barton (2000). This can be seen in the curves and crosses (+) in the lower half of Figure 2: so-called 'unexpected events'. The deceleration gradients (-m) are directly related with the regular Q-value when Q < 1 (see graph, top-left). This example shows application of the low estimated Q-value to estimate (-) m. Width L and potential PR become critical with the 'aggressive' component 3.3.

7 TOO DEEP, HIGH STRESS, FRACTURING

Figures 14 and 15 illustrate the standard approach for estimating the adverse effect of a high ratio of (maximum estimated) tangential stress compared to the uniaxial compression strength σ_c. In fact, this traditional approach has recently been more correctly explained by extensional strain theory (Shen and Barton, 2018, Barton and Shen, 2017). The theory is based on the fact that failure in tension can occur even when all stresses are compressive (Figure 16), due to Poisson's ratio and the stress anisotropy of $\sigma_{\theta\,max} > \sigma_r$. So tensile fracturing occurs first, with propagation of fracturing in shear, if the maximum tangential stress is sufficiently high in relation to the reduced radial stress. The shear failures are unstable and can be dynamic, meaning rock bursting: a very common occurrence with ultra-deep tunnels, with unfortunately a fatal occurrence at Jinping II hydroelectric project in China. The reasons for this will be described later.

Figure 14 (left diagram, from Hoek and Brown, 1980) demonstrates the derivation of the elastic isotr-

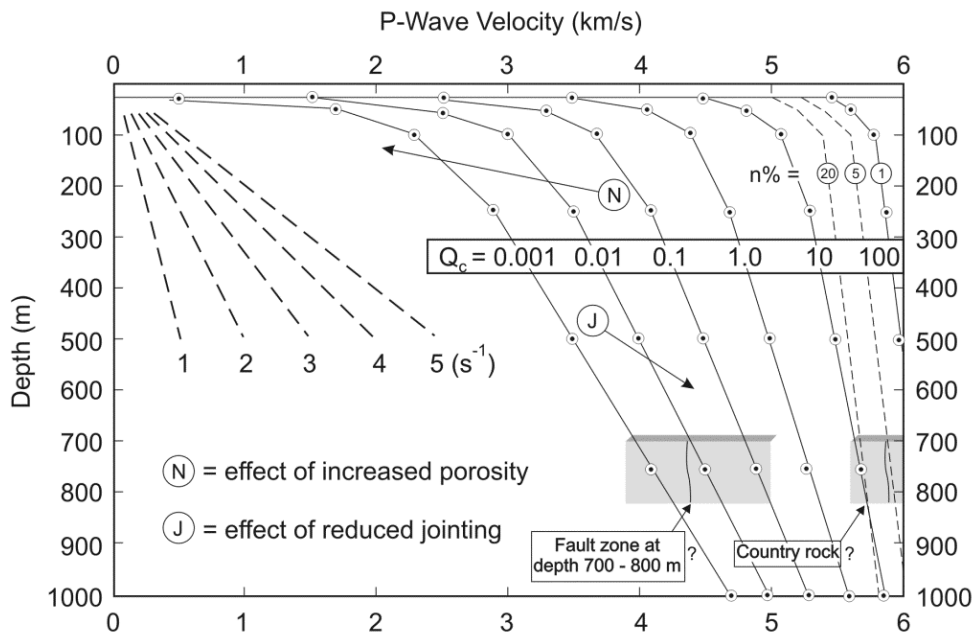

Figure 13. If a highly confined fault zone is remotely sensed ahead of a TBM, its deceptively high P-wave velocity will nevertheless be compromised, when the TBM starts to try to penetrate the zone. Difficult-to-avoid loosening will 'lift' the fault to an equivalent less competent near-surface rock mass performance (i.e. modulus and shear strength reduced, permeability – and water content increased, with V_P maybe reduced to 2 km/s. This, or something similar, has apparently occurred in Figure 11, as the loosened zone has 'expanded' in volume. This of course was not intended.

-opic stress concentration factor, showing 3.0 for a circular opening. Using the estimate of maximum tangential stress ($\sigma_{\theta\,max} = 3\sigma_1 - \sigma_3$) we see that the initiation of fracturing and stress (or strain) induced breakout/overbreak/'dog-earing' begins when the stress /strength ratio reaches 0.4(±0.1). This has been an

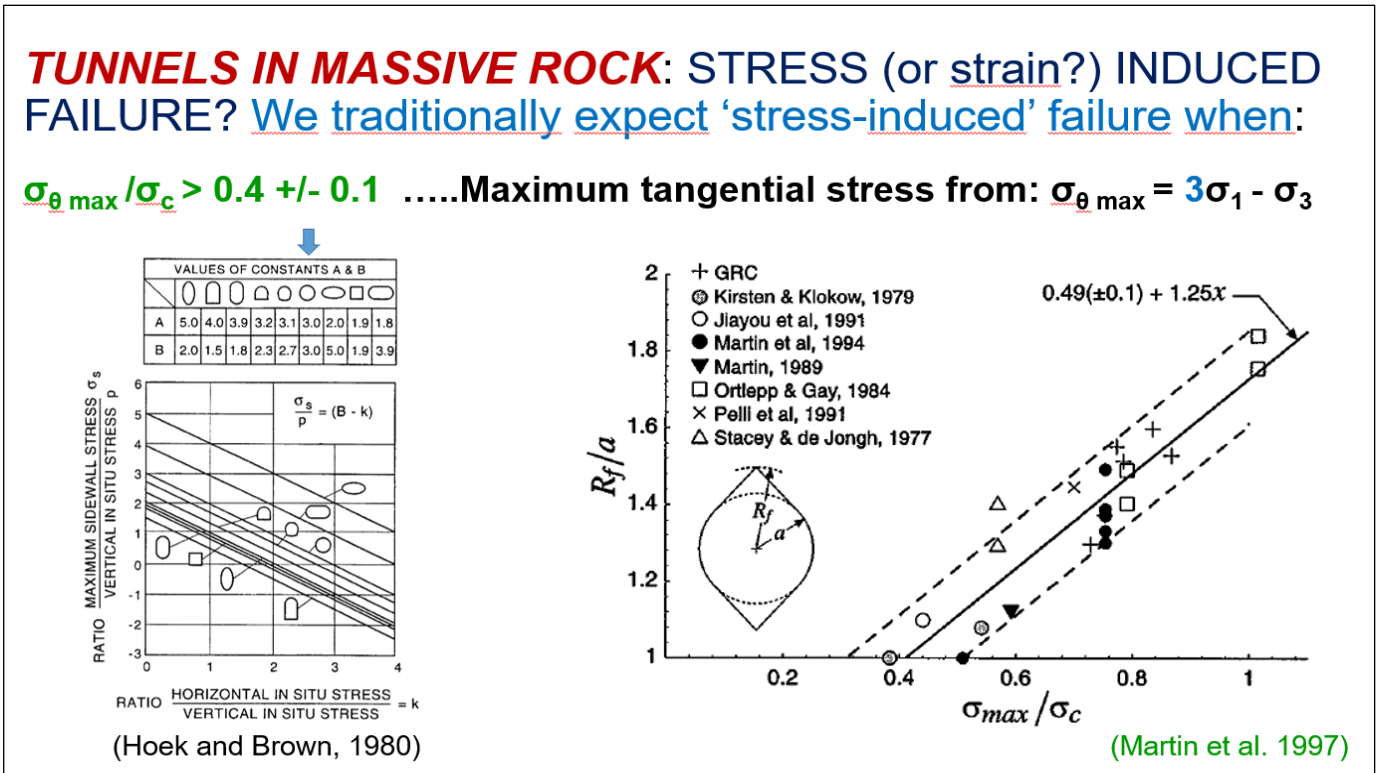

Figure 14. When a TBM tunnel is planned for exceptional depth, such as several kilometers with 2 to 2.5km depth of cover, then it is essential to compare the anticipated maximum tangential stress with the available uniaxial compression strength. Potential depth of failure is shown here. This stress/strength comparison has been the traditional practice when estimating appropriate SRF values, to obtain relevant, heavier tunnel reinforcement using the Q-system, as shown in Table 2.

Table 2. Following the Q-system tunnel support update (from mesh to fibre reinforced shotcrete), Grimstad and Barton (1993) also increased SFR for the case of high-Q massive rock, so that the threat of stress-fracturing would be catered for. As can be noted in the second column of the table, when the stress/strength ratio exceeds 0.4, there is strong acceleration of SRF.

(Table 6b of Grimstad and Barton, 1993)

b) Competent rock, rock stress problems		σ_c/σ_1	σ_θ/σ_c	SRF
H	Low stress, near surface, open joints.	> 200	< 0.01	2.5
J	Medium stress, favourable stress condition.	200-10	0.01-0.3	1
K	High stress, very tight structure. Usually favourable to stability, may be unfavourable for wall stability.	10-5	0.3-0.4	0.5-2
L	Moderate slabbing after > 1 hour in **massive** rock.	5-3	0.5-0.65	5-50
M	Slabbing and rock burst after a few minutes in **massive** rock.	3-2	0.65-1	50-200
N	Heavy rock burst (strain-burst) and immediate dynamic deformations in **massive** rock.	< 2	> 1	200-400

empirical result, independently experienced in mining, nuclear waste disposal research, and in deep road tunnels in Norway, where Grimstad and Barton (1993) utilized accelerated SRF values when this same ratio of stress/strength reaches and exceeds 0.4, as seen in Table 2.

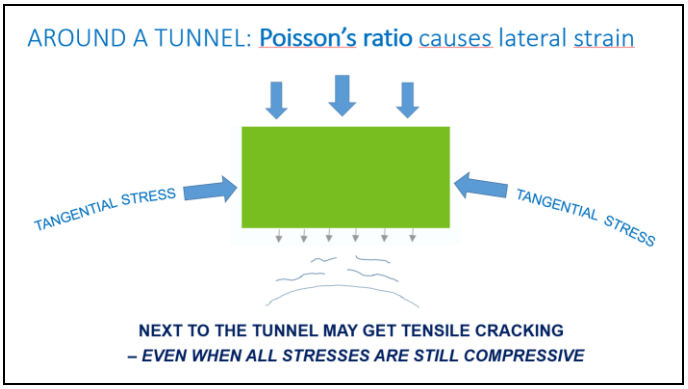

Figure 16. If we turn a uniaxial test sample horizontal (in the case of highest horizontal stress) then Poisson's ratio and the stress anisotropy may cause the critical extension strain to be exceeded in the radial (lateral) direction. Tensile fracturing can therefore occur in the arch (and invert) of the deep tunnel.

The new way of interpreting fracture initiation and propagation pioneered recently by Baotang Shen can be briefly explained by the large-scale 'rotated' uniaxial test specimen shown in green in Figure 16. The important new message is that *Poisson's ratio and a sufficient stress anisotropy allows tensile fracturing to initiate*, despite all principal stresses being compressive. The particularly interesting findings are that both acoustic emission in laboratory tests, and fracture initiation around a deep tunnel, seem to initiate when this 'magic ratio' of 0.4 is reached (the maximum tangential stress divided by the uniaxial compression strength). Figure 17 shows how '0.4' is actually simply explained, with arithmetic.

If stress levels are high enough (if the tunnel is deep enough in massive rock) then fracture propagation will be in the unstable shearing mode, which can be equated with the potential for rock burst.

An example of massive shear failure (with presumed initiation in the tensile mode) is shown by the crushed walls of the 1880 (first significant TBM) Beaumont pilot tunnel, where it passed beneath a 70m high cliff. Fracture mechanics-based modelling with FRACOD is shown in Figures 17 and 18.

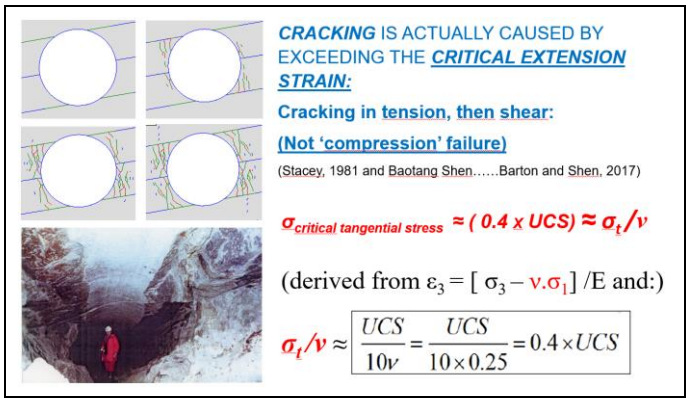

Figure 17. Successive stages of a Baotang Shen FRACOD model, representing the possible progression of tensile to shear fracturing of the 1880 Beaumont tunnel, where this earliest TBM pilot tunnel (for the 110 years later Channel Tunnel) turned under a 70m high cliff. The actual reason for the common fracture initiation stress: 0.4 x UCS is explained. (See Shen and Barton, 2018 for more detail.)

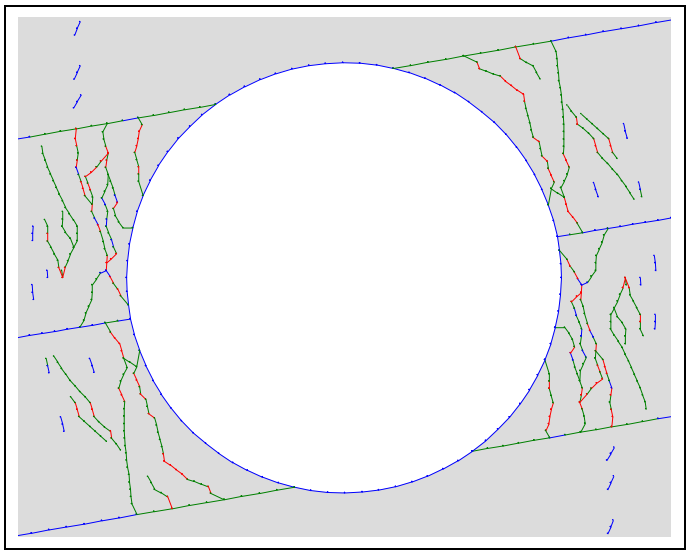

Figure 18. In this model $\sigma_H/\sigma_v = k_0 = 0.33$ has been assumed, which appears as a logical choice in view of the proximity of an adjacent cliff face and sloping shore line. The bedding planes are assumed, based on the single structure seen in the arch in Figure 17. (Note: red = tensile failure, green = shear failure).

Two of the deepest tunnels ever driven by TBM are the 16.7km long headrace tunnels (Figure 19) driven for the Jinping II hydroelectric project. Two of the four parallel 11m diameter tunnels were driven by TBM, two by drill-and-blast. The rock, a medium to high strength marble (approx. 80 to 120 MPa max. 160 MPa) was insufficiently strong to avoid multiple rock-bursting, and eventual *completion of all four* headrace tunnels by drill-and-blast.

Some laboratory test results for the marble (and a weaker schist) were given by Zhang et al. 2011. Figure 18 shows a longitudinal section along these four headrace tunnels (and one fated smaller pilot tunnel). The maximum depth of cover (2.5km) is presently a record for civil engineering, also exceeding the previous deepest: Olmos Tunnel (2.25km) through the Andes in northern Peru.

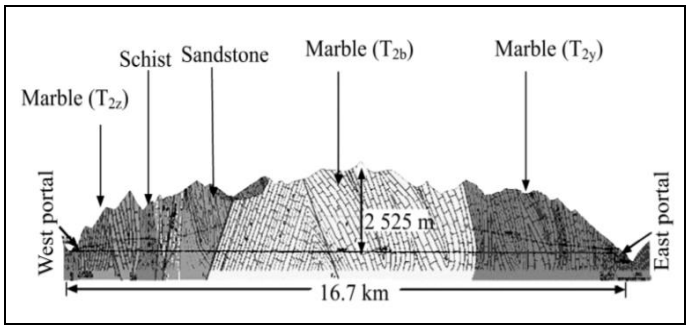

Figure 19. Longitudinal section of Jinping II headrace tunnels. The record depth caused one of the worst TBM rock-burst accidents, due to insufficiently strong marble. Zhang et al. 201

An interesting subject of comparison to Jinping II and the 160km loop in the river from upstream to downsteam, is the Ita HEP 1,400Mw project in south-eastern Brazil. Some details are given in Figure 20. Here the loop in the river was only 11km, and the narrow ridge of rock (< 1km) had ten tunnels: five river diversion, five circular pressure tunnels. All of them were cracked when passing through the most massive (high Q-value) basalt flows. Note Figure 21 effect.

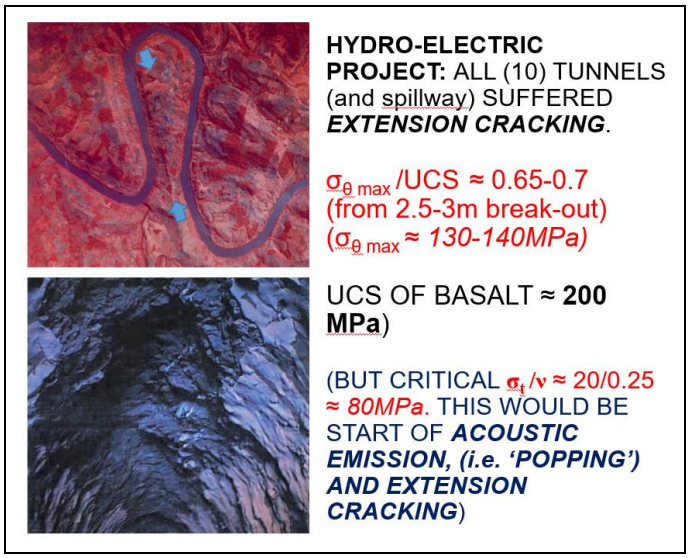

Figure 20. The high stress (and strain) problems experienced at the Ita HEP in Brazil. (Barton and Infanti, 2004). This is used as an illustration of stress/strain induced fracturing, not TBM tunneling. We now need to acknowledge that 0.4 x UCS can be replaced by the ratio of tensile strength and Poisson's ratio σ_t/ν. In this shallow tunnel, extremely high regional stresses were concentrated by the loop in the river. The k_0 ratio of σ_H/σ_v may have beenas high as 20-25, judging by the fractured 200MPa basalt.

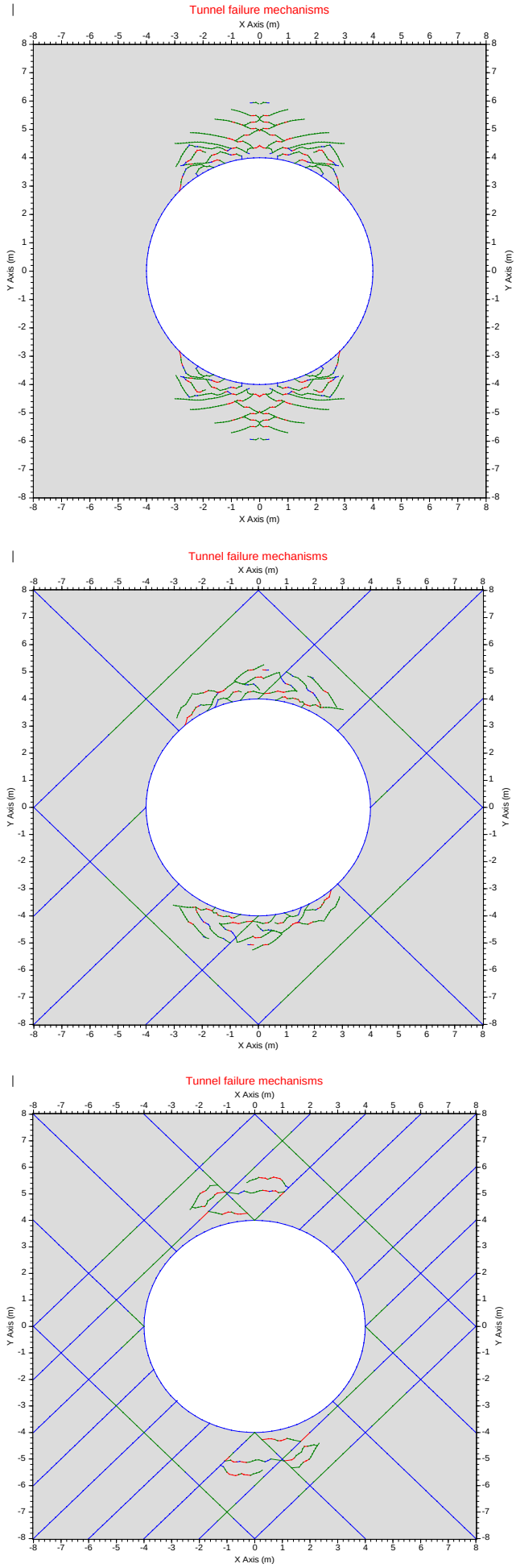

Figure 21 a, b and c. FRACOD modelling by Shen which demonstrate the benefit of jointing when a tunnel is very deep.

8 TOO WET, NEED FOR PRE-INJECTION

Tunnels obviously attract water due to the 'sudden' offer of a huge potential drainage zone which is at atmospheric pressure. In the case of drill-and-blast tunnels it is relatively *easier* to perform high-pressure pre-injection of stabilized, non-shrinking micro-cements with micro-silica additive. Upwards of 40 to 60 25m long holes can be drilled and pre-injected in a 24 to 30 hours operation, when three-to-four boom hydraulic jumbos are used. This assumes that the contractor has been doing this on a continuous basis.

TBM on the other hand have constricted space and the drilling of only 20 holes through pre-formed guide-holes in the front shield may be as much as can be hoped for. If not entirely successful, or if not done, a roughly 10 to 15m length of tunnel is open in front of the last gasketted PC-elements (or shotcreted liner, with less obvious sealing ability). Possible slow progress through this 10 to 15m may allow significant (sometimes tens of litres/sec) inflow and drawdown of groundwater a long way from the TBM.

Figure 22 illustrates situations involving obviously long delays in controlling the water (10,000 hours in the case of the top photo of a karstic inrush of 1m^3/sec, one year *before* this photo was taken).

Figure 22. Water may have a huge impact on TBM progress, and the characterization Jw =0.05, therefore very low effective Q-value may be justified. Bottom photo: Willis, 2012.

9 TBM OR D+B OR HYBRID

In the opinion of the writer, long tunnels should not 'automatically' be considered as candidates for TBM as there are solutions to ventilating drill-and-blast, for example the provision of stiff-tube ducting for vacuum withdrawal of blast gasses. Many – in fact most – assume that TBM will be faster than drill-and-blast for long tunnels Here one needs to be careful. Consider the logic presented in Figures 23, and 24.

Perhaps the 'FF' fault zones are also associated with valleys where intermediate attack points are available for drill-and-blast. Let the TBM bore the better investigated, lower cover section of the project, and use D+B while waiting for TBM delivery. TBM are better when neither very low or very high Q-values are present, as can be seen in the calculations presented in Figure 24. Drill-and-blast progress as a function of Q-value, and TBM as a function of Q_{TBM} are compared.

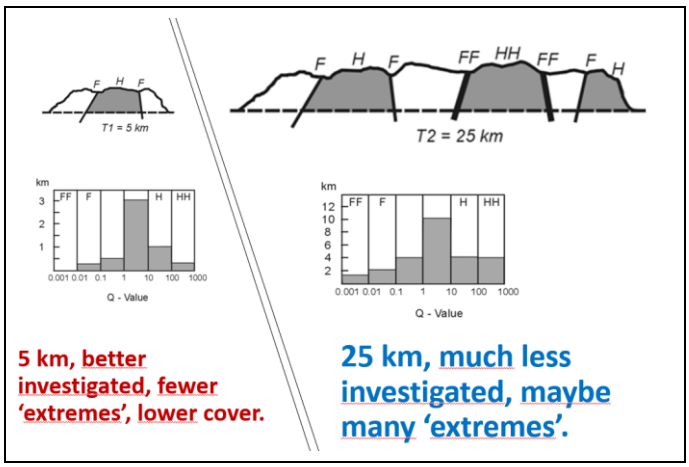

Figure 23. The extremes (at both ends) of the Q-value distribution do not favour the use of TBM. A hybrid solution should be considered, as used several times in China, by design, or by necessity. Barton (2012).

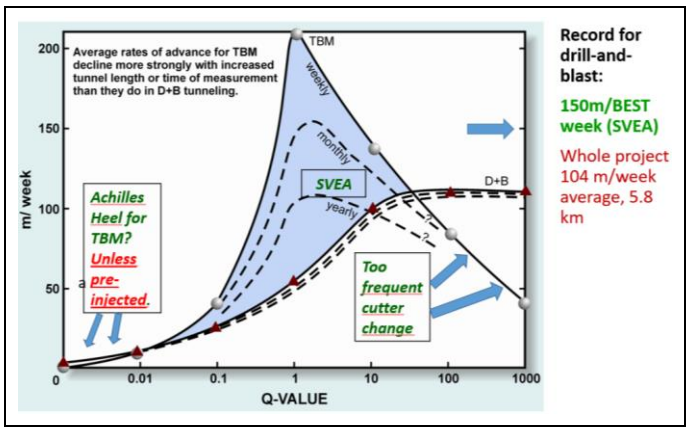

Figure 24. Comparing drill-and-blast with moderately fast TBM over the full range of Q-values with the assumption of neutral (normalized) Q. The best D+B result is indicated. Because of Q-distributions, most D+B may be 40 to 80m/week. Due to 'too-massive', or 'too fractured' zones, four double-shield TBM on one project did not quite reach this moderate TBM prognosis.

10 HARD-ROCK TBM PROGNOSIS

Figure 25 shows a collection of Q-parameter statistics for a hard-rock project in Norway. The statistics apply to the hard-rock exposures (like road and motorway cuttings) in the approximate neighbourhood of the northern 9 to 10 km of a 2 x 19km TBM rail-tunnel project. Unexposed rock and weakness zones are not included. These were measured/investigated with seismic refraction and focussed drilling.

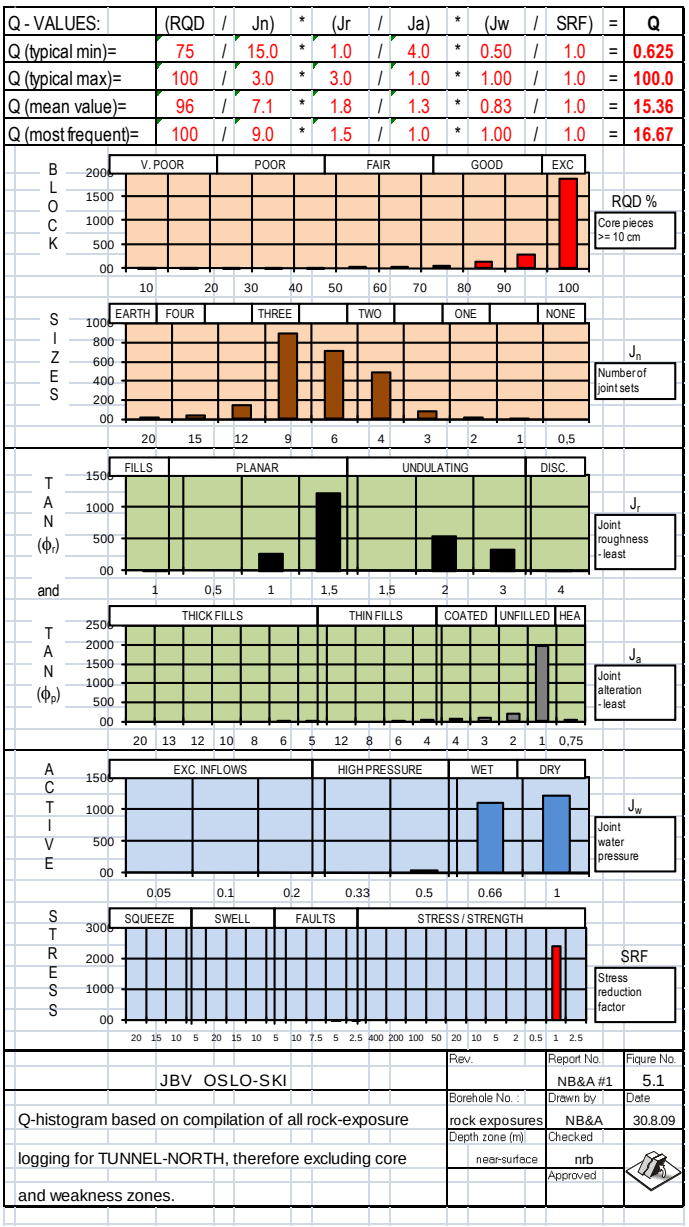

Figure 25. From the near-surface (rock-cutting) observations, and more than 5,000 sets of data, the rock mass appears of ideal quality for drill-and-blast, but not sufficiently jointed (too high RQD) and very hard and abrasive for TBM. Barton and Gammelsæter (2010).

Application of the Q_{TBM} prognosis method can be illustrated by the input data screen shown in Figure 26. This shows the last and most massive assumed Q-class, with assumed Q-parameters of 100/2 x 3/1 x1/1 = 75. This corresponds very well with the majority of shallow refraction seismic V_P values of 5.0-5.5km/s, which converts to approximately Q = 30-100, using the equation $V_P \approx 3.5 + \log_{10} Q_c$ (km/s) suggested by Barton, 2006. If we adjust this for UCS values in the range 100 to 200 MPa, we could suggest a most common range of Q-values of 30 to 50. A majority of the weakness zones had V_P = 2.5-3.0km/s, in other words Q-values down to 0.1, and sometimes lower than this.

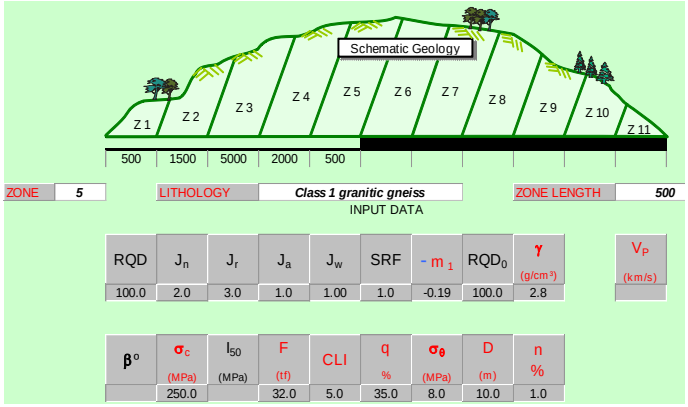

Figure 26. Input data 'screen' for Q_{TBM}, with the parameters assumed for the best Class 5 rock mass. In retrospect, and following more seismic data performed after the prognoses were performed, a greater proportion of this more massive rock than seen in the rock cuttings, would have been used.

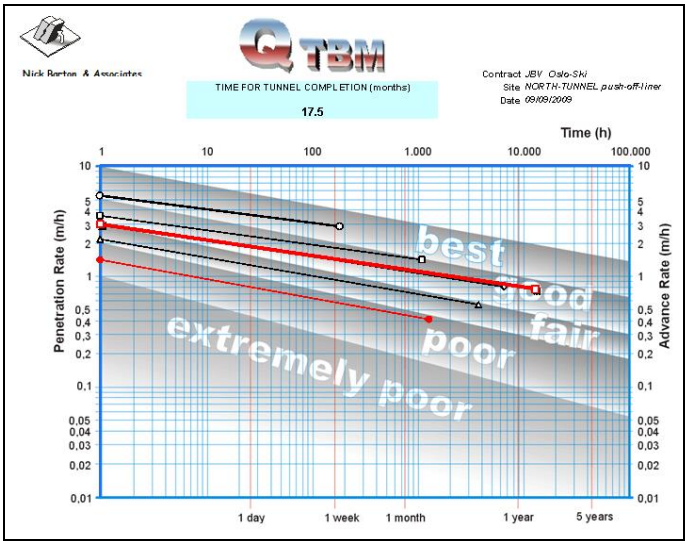

Figure 27. The Q_{TBM} prognosis for the northern pair of tunnels with, in 2009, an assumed length of 9.5km, and application of the double-shield, less negative -m (Table 1).

After just over one year of tunneling (early 2018), the northern TBM have (also, as in Figure 27) both reached the 'g' of good, with average AR of 0.60 m/hr. Mostly, PR have ranged from 1.5 to 2.0m/hr, i.e. on the low side, for reasons connected with hardness, abrasivity, and machine vibration, due particularly to amphibolite fracturing, making 'mixed-face' fall-out along the continuous lenses.

In the case of the highest Q-value rock classes (150, 50 and 16.7) and assumed mean cutter forces of 26 tons, with assumed UCS of 250, 210 and 205 MPa, the predicted PR were 1.4, 2.1 and 3.0 m/hr. The latter

has not been realized, while the two former are more or less as experienced (mean 1.7m/hr).

11 CONCLUSIONS

1. After the learning curve and continued lengthening of the tunnel, TBM tend to decelerate, meaning time-dependent utilization.

2. World record performances show the same deceleration-with-time tendencies.

3. A simple formula that describes why there are delays in low Q-value fault zones has been available for two decades. Improvement of their quality with pre-injection can help here.

4. Of course pre-injection will be needed to control better against groundwater drawdown and settlement damage. TBM may get delayed before the water-tight lining reaches the leaking zone.

5. The assumption of 'stress-induced' fracturing when the estimated maximum tangential stress reaches approx. 0.4 x UCS in deep hard tunnels is standard practice, also for SRF estimation.

6. Recent work by fracture mechanics expert Baotang Shen shows that extension strain caused by Poisson's ratio and anisotropic stress near the tunnel wall causes tensile fracturing. If stresses are very high propagation as unstable shear fractures may cause dynamic events.

7. A simple explanation of the '0.4' factor is now available and also applies to acoustic emission in laboratory testing.

REFERENCES

Barbieri, G, T. Collotta & Tanzini, M. 2013. *Sparvo Highway Tunnel, experiences from the world's largest EPB shield*.

Barton, N. 2000. *TBM Tunnelling in Jointed and Faulted Rock*. Balkema, Rotterdam, 173p.

Barton, N. and Abrahao, R. 2003. Employing the Q_{TBM} prognosis model. *Tunnels and Tunnelling International*, 20-23, December.

Barton, N. 2006. *Rock Quality, Seismic Velocity, Attenuation and Anisotropy*. Taylor & Francis, UK & Netherlands, 729p.

Barton, N. & B. Gammelsæter, B. 2010. Application of the Q-system and Q_{TBM} prognosis to predict TBM tunnelling potential for the planned Oslo-Ski rail tunnels. *Nordic Rock Mechanics Conf.*, Kongsberg, Norway, 56-65.

Barton, N. Reducing risk in long deep tunnels by using TBM and drill-and-blast methods in the same project – the hybrid solution. Keynote lecture. *Risk in Underground Construction. J. Rock Mech. and Geotech. Eng.*, **4**(2): (2012), 115-126, CSRME, Wuhan. Chinese Academy of Engineering.

Barton, N. 2013. TBM prognoses for open-gripper and double-shield machines: challenges and solutions for weakness zones and water. *Fjellsprengningsteknikk, Bergmekanikk, Geoteknikk*, Oslo, 21.1-21.17.

Barton, N. & E. Grimstad. 2014. An illustrated guide to the Q-system following 40 years use in tunnelling. *Web site www.nickbarton.com*, 43 pages, 79 figures and photos.

Barton, N. and Shen, B., 2017. Risk of shear failure and extensional failure around over-stressed excavations in brittle rock.http://dx.doi.org/10.1016/ j.jrmge.2016.11.004. *J. of Rock Mech. & Geotech. Eng*., Vol.9 No. 2, 210-225. Elsevier.

Grandori, R., M. Jaeger, F. Antonini, & L.Vigl. 1995. Evinos-Mornos Tunnel - Greece. Construction of a 30 km long hydraulic tunnel in less than three years under the most adverse geological conditions. *Proc. of Rapid Excavation and Tunnelling Conf. RETC*. San Francisco, 747-767.

Innaurato, N., R. Mancini, E. Rodena, & A. Zaninetti, A. 1991. Forecasting and effective TBM performances in a rapid excavation of a tunnel in Italy. *Proc. 7th ISRM congress, Aachen.* Wittke (ed.) Rotterdam: Balkema. 2:1009-1014.

NTH. 1998. *Full face tunnel boring.* (In Norwegian: Fullprofilboring av tunneler.) Prosjektrapport, anleggsdrift, Trondheim, Norway. 1-94.

Shen, C. P., H.C. Tsai, Y.S. Hsieh & B. Chu. 1999. The methodology through adverse geology ahead of Pinglin large TBM. *Proc. RETC. Orlando, FL*. Hilton & Samuelson (eds). Littleton, CO: Soc. for Mining, Metallurgy, and Exploration, Inc. Ch.8: 117-137.

Shen, B. and N. Barton, 2018. Rock fracturing mechanisms around underground excavations. *Journal of Geotechnical Engineering*, Korea. (in press)

Sundaram, N.M. & Rafek, A.G. 1998. The influence of rock mass properties in the assessment of TBM performance. *Proc. 8th IAEG congress, Vancouver*. Moore & Hungr (eds). Rotterdam: Balkema. 3553-3559.

Willis, D. 2012. TBM probe drilling and pre-grouting – five things to know. *Tunnelling Journal*, July (2012), 43-45.

Zhang, C., w. Chu, N, Liu, Y.Zhu & J. Hou. 2011. Laboratory tests and numerical simulations of brittle marble and squeezing schist at Jinping II hydropower station, China.